J Polym Res (2013) 20:125
DOI 10.1007/s10965-013-0125-5

ORIGINAL PAPER

Swelling/deswelling, thermal, and rheological behavior of PVA-*g*-NIPAAm nanohydrogels prepared by a facile free-radical polymerization method

Marziyeh Fathi · Ali Akbar Entezami · Roghiyeh Pashaei-Asl

Received: 18 November 2012 / Accepted: 15 March 2013 / Published online: 9 April 2013

Abstract A novel method of synthesizing poly(vinyl alcohol)-*g*-*N*-isopropylacrylamide (PVA-*g*-NIPAAm) nanohydrogels under crosslinker-free conditions at high dilution and elevated temperature is presented. Hydrogen peroxide (H_2O_2), used as an initiator, decomposes to hydroxyl radicals at high temperature, which causes the abstraction of hydrogen from PVA chains, resulting in NIPAAm-grafting polymerization. Fourier transform infrared spectroscopy (FT-IR) and thermogravimetric analysis (TGA) confirmed the grafting polymerization of NIPAAm onto PVA chains. The effects of the NIPAAm/PVA feed composition ratio, the amount of H_2O_2, and both pH and temperature on the swelling properties of the nanohydrogels obtained were investigated. An investigation of the swelling/deswelling kinetics and oscillatory swelling behavior of the nanohydrogels indicated that they have high swelling ratios with fast response rates and good reversibilities, and are sensitive to both pH and temperature. Elemental analysis revealed that the NIPAAm content increases with increasing NIPAAm/PVA ratio and H_2O_2 concentration, which leads to a remarkable increase in the nanohydrogel swelling ratio. Rheological studies demonstrated that the samples with higher PVA contents had enhanced elastic responses. The phase-transition temperatures and size distributions of the nanohydrogels were also studied. It appears that that these fast-responding nanohydrogels with properties that are sensitive to both pH and temperature, and which are obtained by a relatively simple and convenient polymerization method, could be potential candidates for drug-delivery carriers.

M. Fathi · A. A. Entezami (✉)
Laboratory of Polymer, Faculty of Chemistry, University of Tabriz, Tabriz, Iran
e-mail: aaentezami@yahoo.com

R. Pashaei-Asl
Faculty of Advanced Biomedical Sciences, Tabriz University of Medical Sciences, Tabriz, Iran

Keywords Nanohydrogels · Cytotoxicity · Thermosensitive · Swelling · Dilution

Introduction

Biocompatible stimuli-responsive nanohydrogels based on *N*-isopropylacrylamide (NIPAAm) are gaining attention due to their numerous potential applications in various biomedical and biotechnological fields, including controlled drug-delivery systems, artificial organs, "on–off" switches, and so on [1–5]. It is well known that aqueous poly(*N*-isopropylacrylamide) (PNIPAAm) solution exhibits a lower critical solution temperature (LCST) of approximately 32 °C. When the temperature of its environment is below the LCST, PNIPAAm absorbs a large amount of water and exhibits a swollen and hydrophilic state. Above the LCST, it demonstrates abrupt volume shrinkage and becomes hydrophobic due to the expulsion of free water inside the polymer network [6, 7]. A fast response to the ambient temperature is one of the most important characteristics required for the applications mentioned above, but conventional PNIPAAm hydrogels form a dense, thick skin layer that restricts their response rates and results in low reswelling and deswelling rates [8, 9]. Therefore, it is necessary to modify PNIPAAm hydrogels in order to meet the requirements of practical applications. Many strategies have already been proposed to promote the response rates of PNIPAAm hydrogels.

Decreasing the size of the hydrogel is considered to be the best way to obtain products with sufficient response times. In other words, the slow dynamics of the swelling/deswelling process in macroscopic hydrogels can be overcome and accelerated by preparing nanohydrogel particles with dimensions in the submicrometer range, because the response time of hydrogel swelling/deswelling is proportional to the linear size of the hydrogel [8, 10, 11]. Precipitation and emulsion

polymerization are the techniques most commonly employed to synthesize thermosensitive nanohydrogels. However, these methods involve the use of surface-active and crosslinking agents that can be expensive, have limited particle size distributions, and can be toxic [12–14]. On the other hand, Gao and Friskin have reported that it is possible to make PNIPAAm microgels without using any crosslinker by precipitation polymerization through a chain-transfer reaction via tertiary carbon both during and after the polymerization of NIPAAm monomers [15, 16]. Also, radiation polymerization makes it possible to form nanoparticles or nanohydrogels from linear polymers in dilute aqueous solution under additive-free conditions through intra/interchain collapse, which can be applied as a facile method to make well-defined, biocompatible delivery vehicles [17–20]. Furthermore, many investigations have been performed to synthesize PVA/PNIPAAm interpenetrating (IPN) and semi-interpenetrating (semi-IPN) polymeric networks as macroscopic gels with enhanced response times and mechanical strengths via radical polymerization in the presence of crosslinking agents [9, 21, 22]. This is because responsive polymers like PNIPAAm have poor biocompatibilities, mechanical strengths, and swelling–deswelling rates [23], whereas PVA is a nontoxic, linear, water-soluble polymer with high hydrophilicity and good biocompatibility, so copolymers of PNIPAAm and PVA could potentially combine the desirable properties of both, including the biocompatibility and mechanical strength of PVA [9]. In the work described in the present paper, a novel method for the preparation of nanohydrogels of NIPAAm based on the intramolecular collapse method under diluted conditions was developed. In this approach, NIPAAm is grafted onto biocompatible linear PVA chains via free-radical polymerization at the boiling point of water in very dilute solution, using hydrogen peroxide (H_2O_2) as an initiator. PVA-*g*-NIPAAm nanohydrogels were synthesized with different NIPAAm/PVA feed ratios and H_2O_2 concentrations. The structures, compositions, thermal stabilities, rheological behaviors, cytotoxicities, and phase-transition temperatures of the nanohydrogels obtained were then analyzed. Their swelling properties, such as the variations in their equilibrium swelling ratios with temperature and pH, their deswelling kinetics, and their oscillatory swelling in water, were also studied.

Experimental

Materials

NIPAAm (Acros Organics, Geel, Belgium) was used without further purification. A dialysis membrane (benzoylated dialysis tubing, molecular weight cutoff 2000) and PVA (average molecular weight 1.95×10^5, degree of saponification 98 mol%) were purchased from Aldrich (St. Louis, MO, USA). Also, H_2O_2 30 % (Scharlau, Barcelona, Spain) was employed as an initiator, and was used as received.

Preparation of PVA-*g*-NIPAAm nanohydrogels

The PVA-*g*-NIPAAm nanohydrogels were synthesized by free-radical polymerization in very dilute solution at elevated temperature through intramolecular crosslinking. The PVA was dissolved in deionized water and heated to the boiling point of water for 1 h to achieve the desired aqueous solution. The PVA solution was mixed with NIPAAm and the mixture was stirred under an argon atmosphere in a 250-mL two-necked flask for 30 min at boiling point of water. A degassed aqueous solution of H_2O_2 was added to the flask to initiate polymerization. The reaction system was stirred at the incubation temperature (boiling point of water) for 1 h. Table 1 lists the labels and feed composition ratios of the resulting nanohydrogels. After polymerization, the final white dispersion was cooled to room temperature. In order to remove unreacted NIPAAm monomer, the dispersion was then purified by performing dialysis against deionized water at room temperature with a dialysis membrane (molecular weight cutoff 2000). The deionized water was replaced every 8 h. After that, the nanohydrogel dispersions obtained were freeze-dried. To eliminate the homo-PNIPAAm, which is soluble in water below the LCST [24], the dried nanohydrogels were immersed in deionized water at room temperature. The water was changed repeatedly until the external solution did not show a phase transition at temperatures above the LCST. Finally, to remove any sol fractions of PVA that were not incorporated into the crosslinked network, the nanohydrogels were soaked in hot water and the purified nanohydrogels were lyophilized again. Crosslinked PVA and PNIPAAm nanohydrogels were synthesized by the same polymerization method to compare some of their properties with those of the PVA-*g*-NIPAAm nanohydrogels.

Table 1 Feed composition ratios of the various nanohydrogels obtained in this work

Nanohydrogel label	wt.% of NIPAAm	wt.% of PVA	H_2O_2 (μL)
NHG1	1	0.5	10
NHG2	1	1	10
NHG3	1	2	10
NHG4	1	1	20
NHG5	1	1	30
NHG6	-	1	10
NHG7	1	-	10

FT-IR characterization of nanohydrogels

A Tensor 27 Fourier transform infrared (FT-IR) spectrophotometer (Bruker, Ettlingen, Germany) was employed to obtain nanohydrogel spectra. These FT-IR spectra were utilized to confirm the incorporation of NIPAAm into the polymer network.

Determination of nanohydrogel composition

Elemental analysis was carried out on freeze-dried nanohydrogels using an Elementar (Hanau, Germany) vario MAX instrument. The NIPAAm content of each nanohydrogel was estimated by performing an elemental analysis of the nitrogen content.

Dynamic light scattering (DLS) measurement

DLS was used to determine the particle sizes and the particle size distributions of the synthesized PVA and PVA-*g*-NIPAAm nanohydrogels in solution. Before performing the measurements, 1 mg/ml of the dried product was sonicated for 30 s. The DLS measurements were attained below the LCST (at 25 °C) using a DLS instrument (Malvern Instruments, Malvern, UK) equipped with an argon laser operating at 632.8 nm with a fixed scattering angle of 90°.

Calorimetric measurements

The DSC measurements were conducted using a Netzsch (Selb, Germany) DSC 200 instrument under an N_2 flow at a heating rate of 1 °C/min, with the temperature ranging from 20 to 50 °C. The samples were wetted beforehand in distilled water at room temperature to reach the equilibrium swelling ratio. All samples were blotted free of water using filter paper prior to the DSC measurements. The LCSTs were derived from the onset point of the endothermic DSC peak.

Thermogravimetric studies

Thermogravimetric (TG) and differential thermogravimetric (DTG) curves of nanohydrogels were obtained using a thermogravimetric analyzer (TGA 1750, Linseis, Selb, Germany) by heating from room temperature to 700 °C at a heating rate of 10 °C/min under a nitrogen flow. The mass of the sample pan was recorded continuously as a function of temperature.

Rheological measurements

The storage moduli (G') and the loss moduli (G'') of the hydrated nanohydrogels were measured using a parallel-plate rheometer (MCR-301, Anton Paar, Graz, Austria) as a function of the frequency. The swollen nanohydrogels were placed between the parallel-plate rheometer with a diameter of 40 mm and a gap of 1.0 mm. Dynamic frequency sweep tests were performed from 0.1 to 100 rad/s at 20 °C with a strain amplitude of 0.2 %, which is within the linear viscoelastic region as determined by a dynamic strain sweep. The dynamic strain sweep test was performed from 0.1 to 100 % strain with a frequency of 1 rad/s at 20 °C.

Swelling/deswelling kinetics

The progress of the swelling process was monitored gravimetrically [25, 26]. To measure the swelling kinetics, preweighed nanohydrogels were immersed in distilled water at 25 °C. After excess surface water had been removed with filter paper, the weight of the swollen sample was measured at various time intervals. The swelling ratio (SR, %) of the hydrogel was defined using the following equation:

$$SR(\%) = ((W_s - W_d)/W_d) \times 100,$$

where W_s is the weight of the swollen hydrogel at a predetermined time and W_d is the dry mass of the hydrogel.

The deswelling kinetics of the nanohydrogels were followed by performing gravimetric measurements of the weight of water in the nanohydrogel (W_t) at specific time intervals after the swollen gel at 6 °C had been quickly transferred to hot water at 45 °C. The water retention (WR) was calculated as

$$WR(\%) = ((W_t - W_d)/(W_s - W_d)) \times 100.$$

Reversibility of rapid swelling/deswelling kinetics

An oscillatory swelling study was carried out in water at alternating temperatures between 20 °C and 42 °C. The nanohydrogel samples were maintained for 5 min at 20 °C to achieve the equilibrium swelling ratio, and were then placed in water at 42 °C for 5 min to shrink them. The weights of the samples were measured gravimetrically, and the deswelling and reswelling measurements were repeated several times.

Temperature and pH dependences of the swelling ratio

A swelling study was conducted on the nanohydrogels to investigate the behavior of the swelling ratio as a function of the temperature and pH in the swelling medium. The equilibrium swelling ratio (ESR) was calculated from gravimetric measurements of dry nanohydrogels (W_d) and nanohydrogels immersed in water

for 24 h (W_e) at different temperatures (6–45 °C) or buffer solutions (pH 2–10). The equilibrium swelling ratio was calculated using the following formula:

$$ESR(\%) = ((W_e - W_d)/W_d) \times 100,$$

where W_e is the weight of the swollen state.

Cell culture

A549 cells (adenocarcinomic human alveolar basal epithelial cells) were grown in a 25 cm^2 flask (Orange Scientific, Braine-l'Alleud, Belgium) in RPMI-1640 (Roswell Park Memorial Institute 1640) medium (Gibco, Invitrogen, Carlsbad, CA, USA) supplemented with 10 % fetal bovine serum (FBS) (Gibco, Invitrogen), penicillin (100 unit/ml) (Sigma, St. Louis, MO, USA), and streptomycin (100 μg/ml) (Sigma), and incubated at 37 °C in a 5 % CO_2 humidified atmosphere.

Cell cytotoxicity assay

A cytotoxicity study was done to evaluate the effect of the nanohydrogel NHG3 (as an example of a typical synthesized nanohydrogel) on cell survival. When the cells reached 80–90 % confluency in the flask, they were washed in PBS solution (Sigma) and harvested via treatment with 0.05 % trypsin/EDETA (Gibco, Invitrogen). The live A549 cells were counted and almost 7,000 cells were seeded per well in 200 μl of growth medium in a 96-well flat-bottomed tissue culture plate (TPP, Trasadingen, Switzerland) and incubated at 37 °C and 5 % CO_2 in an incubator overnight. The next day, the medium was removed and the cells were washed with PBS solution and treated with various concentrations (60–250 ppm) of nanohydrogel before being incubated for 24 h at 37 °C in the presence of 5 % CO_2. In addition, an untreated culture was incubated for use as a control sample. The cell viability was determined using an MTT (3-(4,5-dimethylthyazol-2-yl)-2,5-diphenyltetrazolium bromide) assay; 50 μl/ml of MTT (Sigma) solution with 150 μl of media were added to each well and incubated for 4 h at 37 °C. After incubation, the medium was removed and a mixture of 200 μl of DMSO (dimethyl sulfoxide) and 25 μl of Sorenson's buffer was added to each well to solvate the blue formazan crystals. The optical density (OD) was then measured at 570 nm with a microplate reader (Awareness Technology, Palm City, FL, USA). The OD of the control sample was normalized to 100 %. The viable rate was calculated using the following equation:

$$Viable\ rate = \left(OD_{(treatment)}/OD_{(control)}\right) \times 100.$$

The OD of the treated sample was measured in the presence of nanohydrogel while the OD of the control sample was measured in the absence of nanohydrogel. Each experiment was repeated in triplicate, and the results were expressed as the mean±standard deviation (SD).

Results and discussion

Preparation of PVA-*g*-NIPAAm nanohydrogels

Using radiation processing technology [17–20, 27, 28], nanohydrogels have been synthesized through intramolecular crosslinking with linear water-soluble polymers such as PVA, poly(vinylpyrrolidone) (PVP), poly(acrylic acid) (PAAc), and poly(vinyl methyl ether) (PVME) without any in situ monomer polymerization and grafting. While this method does not require an initiator, catalyst, or crosslinker, it does require a high dose of ionizing radiation (tens or hundreds of kGy). Therefore, in this work, we attempted to design a new method of synthesizing PVA-*g*-NIPAAm nanohydrogels by free-radical polymerization based on the intramolecular crosslinking of PVA chains in dilute solution, using a similar approach to that employed in irradiation polymerization. As a result, free radicals of PVA in dilute aqueous solution were obtained by applying H_2O_2 at the boiling point of water, which causes H_2O_2 to decompose into hydroxyl radicals. Hydroxyl radicals generated from the decomposition of H_2O_2 initiate the polymerization of NIPAAm (homo-PNIPAAm) as well as the grafting reaction (through the abstraction of H atoms from PVA chains) in a random manner [29, 30]. It is assumed that this reaction leads to PVA with a branched structure involving growing chains of PNIPAAm. In a dilute homogeneous solution (with each macromolecule separated) of PVA, polymerization proceeds through reactions such as intramolecular crosslinking between the growing chains of PNIPAAm on PVA, free radical attack on PVA, and the growth of PNIPAAm chains in solution. These reactions result in gels with crosslinked structures and lead to nanohydrogel formation. On the other hand, at high temperatures (higher than the LCST), PVA-*g*-NIPAAm forms nanohydrogels that are physically crosslinked via the hydrophobic nanodomains generated by dehydrating PNIPAAm [31]. Scheme 1 shows a schematic representation of nanohydrogel preparation. Therefore, in this work, different PVA-*g*-NIPAAm nanohydrogels were prepared by tailoring the NIPAAm/PVA feed ratio and H_2O_2 concentration. It is worth mentioning that a white dispersion is obtained after polymerization. To obtain the dry nanohydrogel, this dispersion was freeze-dried (lyophilized). A significant change in the structure of PVA-*g*-NIPAAm occurs during the freezing process. The formation of gel-like structures after the freezing–thawing of polymer dispersions has been reported. This structural densification occurs due to the formation of a supermolecular and

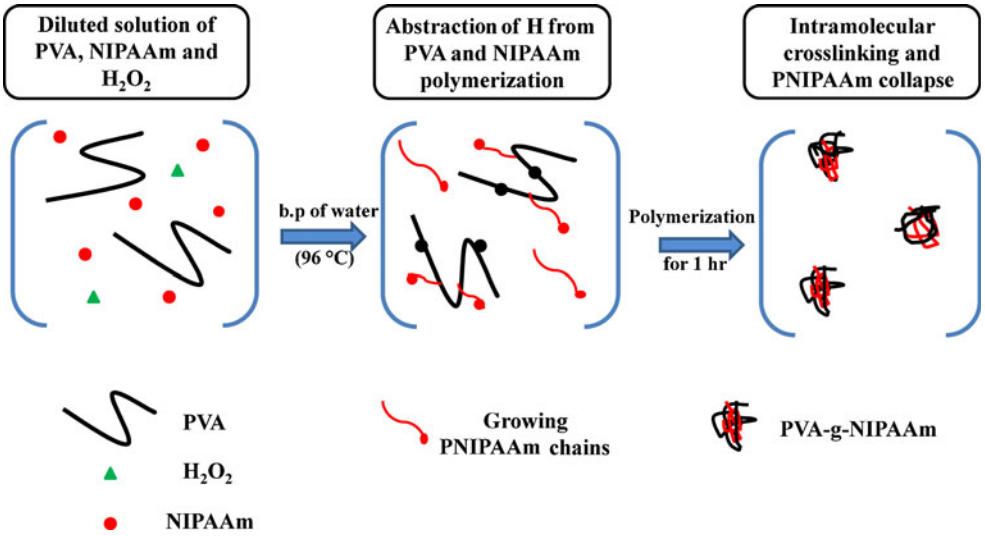

Scheme 1 Schematic illustration of PVA-*g*-NIPAAm nanohydrogel preparation

semicrystalline structure [32], which can be attributed to the formation of some hydrogen bonds at the ends of the PVA chains, because the PVA chain activity decreases during the freezing process [33, 34]. After the synthesized dispersion has been freeze-dried, the product obtained is a compact white nanohydrogel that can swell extensively in water without dispersion. As a result, it is possible to use gravimetric measurements and filter-paper wiping in swelling experiments.

FT-IR analysis

FT-IR spectra of PVA and PVA-*g*-NIPAAm nanohydrogels were used to confirm the occurrence of grafting polymerization. Figure 2 shows the FT-IR spectra of PVA nanohydrogel (a) and PVA-*g*-NIPAAm nanohydrogels (b). In the PVA nanohydrogel spectrum, the broad band at about 3430 cm^{-1} is assigned to the stretching of intermolecular and intramolecular O–H hydrogen bonds. The band observed at around 2930 cm^{-1} relates to the stretching of C–H bonds in alkyl groups, while the peaks between 1710 and 1650 cm^{-1} are due to the stretching of C=O bonds in the remaining acetate groups from PVA (saponification reaction of polyvinyl acetate) [35]. The FT-IR spectrum of the PVA-*g*-NIPAAm nanohydrogels (b) show peaks from –NH in the PNIPAAm component and from the stretching of –OH in PVA at around 3400 cm^{-1}. The peaks at 2900 cm^{-1} are due to the stretching of C–H bonds on the PVA and PNIPAAm backbone. Amide I and amide II bands are observed at 1644 cm^{-1} and 1553 cm^{-1}, respectively; these arise from the amide group of the PNIPAAm component. A peak at 1459 cm^{-1} and a doublet at 1378 cm^{-1} are due to two $–CH_3$ bonds in the PNIPAAm side chains [36]. Thus, Fig. 1 shows that the spectrum of the PVA-*g*-NIPAAm nanohydrogels includes all of the peaks expected from both the PVA and the PNIPAAm components.

Elemental analysis of nanohydrogels

After purification, the PNIPAAm contents of the resulting nanohydrogels were determined by performing an elemental analysis of their nitrogen contents. The results obtained are summarized in Table 2. It is clear that the PNIPAAm contents of NHG1–3 decrease with decreasing NIPAAm content in the initial feed. Also, increasing the amount of initiator increases the PNIPAAm content. As shown in Table 2, the NIPAAm content in the nanohydrogels (NHG1, NHG4, and NHG5) tends to increase with increasing initiator concentration. Increasing the concentration of the initiator increases the probability of hydrogen abstraction from the PVA backbone and NIPAAm graft polymerization. Furthermore, the PNIPAAm content in the nanohydrogel is lower than that in the initial feed. This is due to the formation of homo-PNIPAAm during grafting polymerization and the subsequent removal of unreacted monomers during the purification process.

TG and DTG determination of nanohydrogels

The TG and DTG thermograms of PNIPAAm, PVA, and the nanohydrogels NHG1–2 are depicted in Fig. 2. Figure 2a shows that PNIPAAm presents one-stage degradation behavior at 400 °C. As shown in Fig. 2c, the first-derivative curves of the PVA nanohydrogels show two degradation peaks due to variations in the molecular weight of the polymer used [37]. However, the grafting of NIPAAm onto PVA affects its thermal properties. PVA-*g*-NIPAAm nanohydrogels exhibit faster thermal decomposition than PVA nanohydrogels because of the introduction of PNIPAAm (Fig. 2b) [38]. The difference between the thermal stabilities of PVA and PVA-*g*-NIPAAm confirms that the reaction products are graft copolymers.

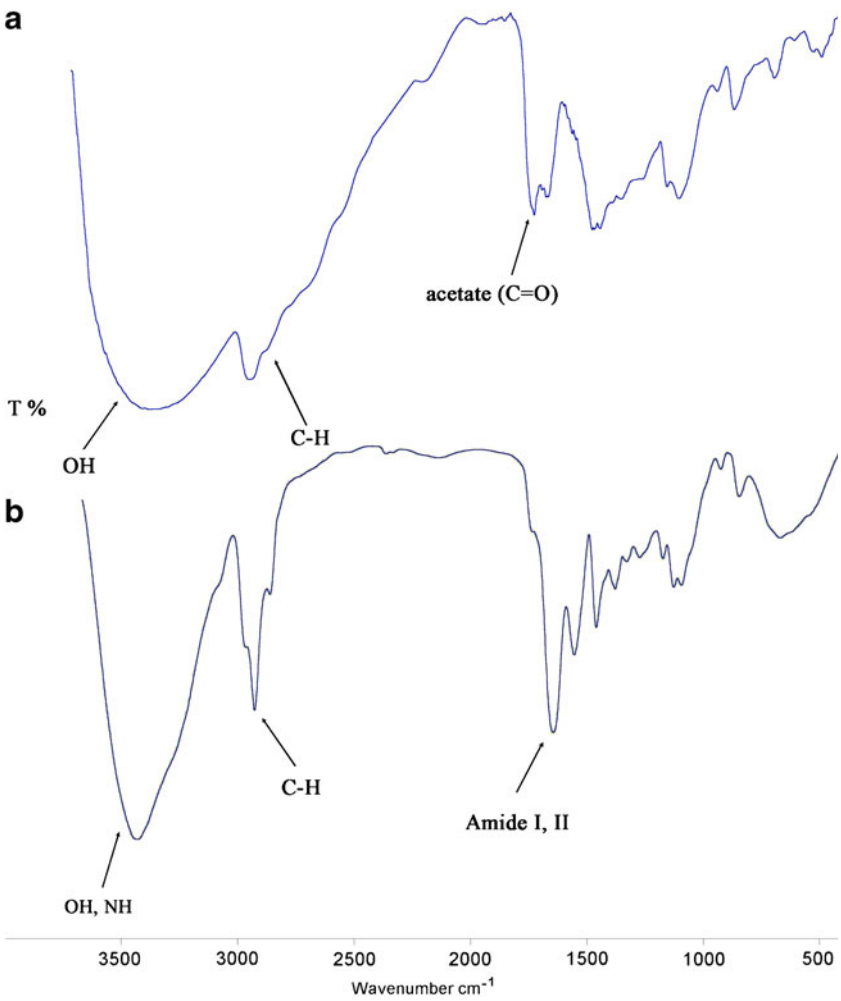

Fig. 1a–b FT-IR spectra of PVA **a** and PVA-*g*-NIPAAm **b** nanohydrogels

Size distributions of the nanohydrogels

The mean particle sizes and the size distributions of the PVA and PVA-*g*-NIPAAm nanohydrogels were determined via DLS at 25 °C. For the DLS measurements, the nanohydrogels (at a concentration of 1 mg/mL) were sonicated for 30 s to disperse them in deionized water. As shown in Fig. 3, the DLS diagram of the PVA-*g*-NIPAAm nanohydrogel NHG3 (used here as a representative synthesized nanohydrogel) indicates a narrow size distribution with an average diameter of about 80 nm. Also, the DLS diagram of the PVA nanohydrogel NHG6 shows a very small particle size of around 18 nm. It is therefore obvious that the grafting of NIPAAm onto PVA chains leads to an increase in the size of the nanohydrogel.

LCSTs of the nanohydrogels

The LCSTs of the water-swollen homo-PNIPAAm (NHG7) and PVA-*g*-NIPAAm nanohydrogels (NHG1–3) were measured by DSC. Figure 4 indicates that the LCST of the homo-PNIPAAm is around 29 °C, while the LCSTs for the PVA-*g*-NIPAAm samples are approximately 30 °C (based on the onset temperature of the endothermic peak). Thus, the phase transition temperatures of the PVA-*g*-NIPAAm nanohydrogels are very similar to that of the homo-PNIPAAm, which may be attributed to the hydrophilicity of PVA [39]. Also, Fig. 4 shows that nanohydrogels with different NIPAAm/PVA ratios have nearly the same LCST. These results imply that the interaction between the PVA backbone and the PNIPAAm chains can be neglected.

Rheological behavior

A gel (elastic solid) can be defined based on the concept that the storage modulus (G') is dominant in the gel phase while the loss modulus (G'') is dominant in the sol phase [21]. The frequency dependences of the storage and loss moduli were determined using a strain amplitude of 0.2 %, as shown in Fig. 5 for swollen NHG1–3. The samples behaved as viscoelastic solids, and the storage modulus was larger than the loss modulus across the entire frequency range, which is a characteristic feature of crosslinked hydrogels [21, 40–43].

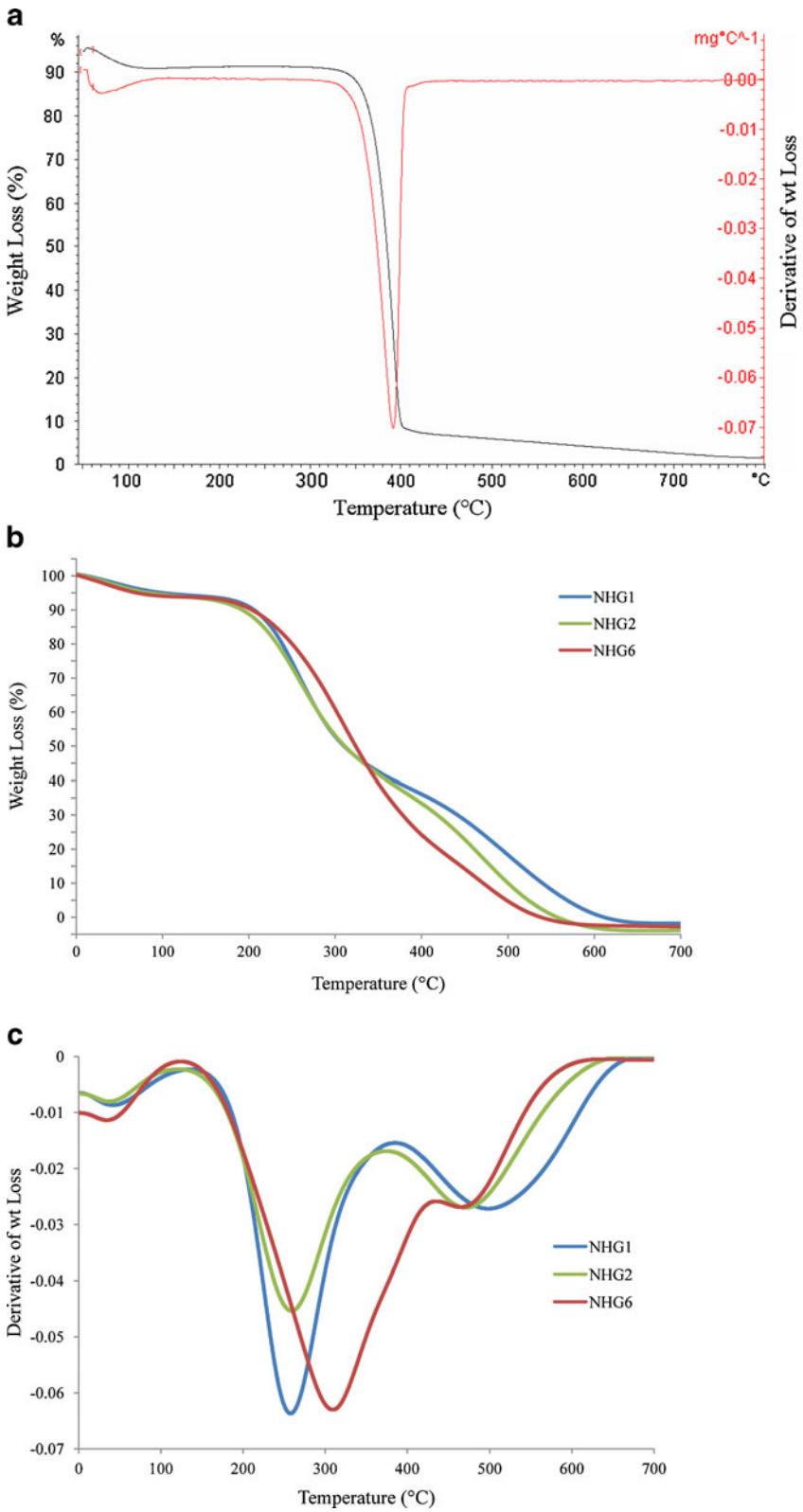

Fig. 2a–c TG and DTG curves of NHG7 (**a**); TG curves of nanohydrogels NHG1–2 and NHG6 (**b**); DTG curves of nanohydrogels NHG1–2 and NHG6 (**c**)

Furthermore, the results of the dynamic frequency sweep measurements of the swollen samples showed a marked increase in the modulus with increasing PVA content in the samples. This can be attributed to the more compact and complex structures of the samples with high amounts of PVA, which enhanced the visco-elastic properties. Also, all of the nanohydrogels obtained by intramolecular crosslinking in this work

Table 2 NIPAAm contents of the nanohydrogels, as determined by nitrogen elemental analysis

Sample label	NIPAAm in initial composition (wt./wt.%)	H_2O_2 (μL)	H (%)	C (%)	N (%)	NIPAAm in final matrix (wt./wt.%)
NHG1	66	10	8.6	54.9	8.1	51.33
NHG2	50	10	8.8	54.6	4.4	19.1
NHG3	33	10	9.0	55.3	3.4	13
NHG4	50	20	8.7	54.8	5.2	24.2
NHG5	50	30	8.9	56.4	7.3	39.9

had high elastic moduli that were comparable with those obtained using a crosslinking agent.

Effect of PVA content on the swelling/deswelling behavior

The most important property of hydrogels is their swelling behavior, which is usually monitored via gravimetric measurements of water uptake. Figure 6 shows the swelling kinetics of NHG6 (homo-PVA nanohydrogel) in comparison with the nanohydrogels NHG1–3, which were synthesized with PVA contents of 0.5, 1, and 2 wt. %, respectively. As illustrated in Fig. 6, the synthesized NHG1–3 showed very fast water uptake and high degrees of swelling within several minutes. The fast swelling rates of the synthesized PVA-*g*-NIPAAm nanohydrogels are due to several important factors. As the response time for hydrogel swelling/deswelling is proportional to the square of the linear dimension of the hydrogel [6], the nanoscale nature of the synthesized PVA-*g*-NIPAAm hydrogels results in a faster response time. Also, the introduction of PVA chains exerts a great influence on the swelling rates of the synthesized nanohydrogels. In addition, in the method that we utilized, the nanohydrogels form at the boiling point of water, and preparing the gels at temperatures above the LCST results in a phase-separated structure, which can greatly enhance the response rate [44]. On the other hand, it was observed that the ESRs of the PVA-*g*-NIPAAm nanohydrogels were much higher than the ESRs of the PVA nanohydrogels, indicating that the grafting of NIPAAm onto PVA leads to a considerable increase in the swelling ratio because of the hydrophilicity of NIPAAm [22]. In line with this concept, the swelling ratios of the synthesized nanohydrogels increase with increasing NIPAAm content in the nanohydrogel (according to elemental analysis results: see Table 2), so NHG1 (which has the highest NIPAAm content) exhibits the highest swelling ratio. Furthermore, NHG1–3 show very fast deswelling kinetics, as depicted in Fig. 7. The swollen nanohydrogels at 6 °C were placed in water at 45 °C and their subsequent deswelling behavior was recorded. The nanohydrogels collapsed within seconds, squeezing out 50–75 % of the water within them within 2 min. NHG1 (which had the highest content of PNIPAAm) pushed out 75 % of its water, while NHG2 and NHG3 lost about 62 and 50 % of their water, respectively. These results confirm that a high PNIPAAm content leads to more swelling.

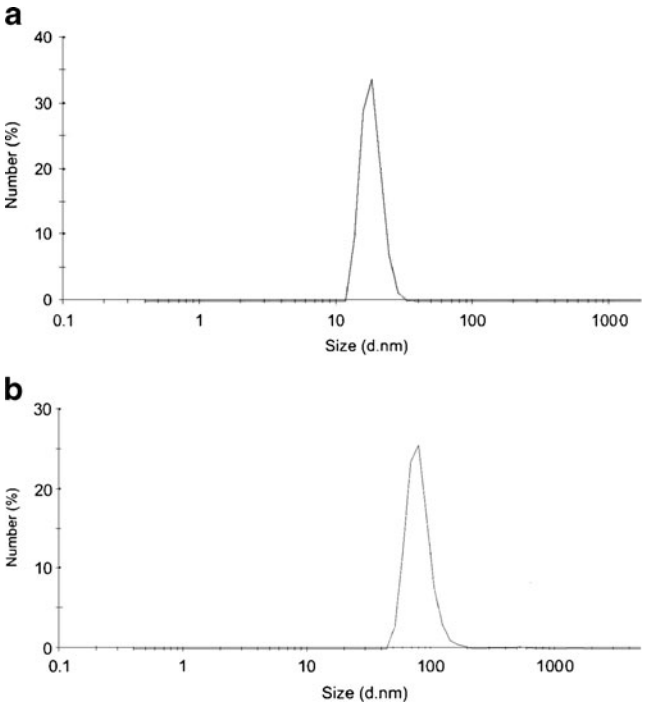

Fig. 3a–b Size distributions of the PVA (**a**) and PVA-*g*-NIPAAm (**b**) nanohydrogels

Oscillatory swelling kinetics of the nanohydrogels

To develop a hydrogel for use as an artificial muscle and in pulsed drug delivery, it is important to achieve reversibility of the rapid swelling/deswelling process [45]. The oscillatory swelling of nanohydrogels NHG1–3 was studied by applying 5-min temperature cycles between 20 °C and

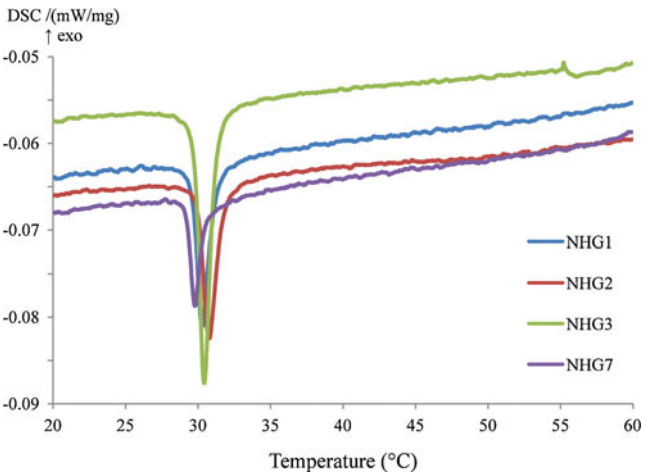

Fig. 4 DSC thermograms of NHG1–3 and NHG7

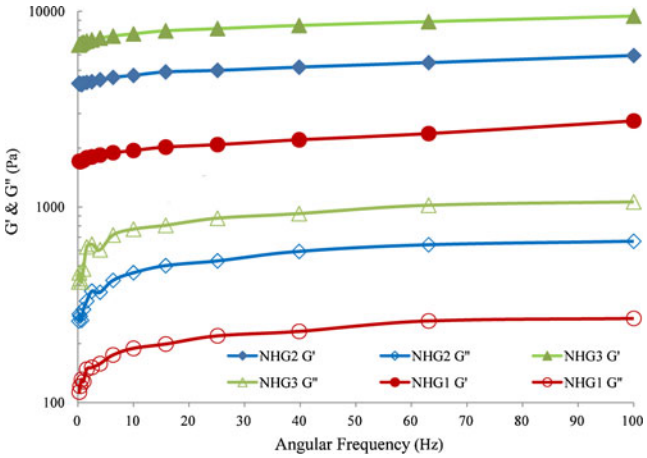

Fig. 5 Frequency dependences of the elastic (G') and viscous (G'') moduli of nanohydrogels NHG1–3

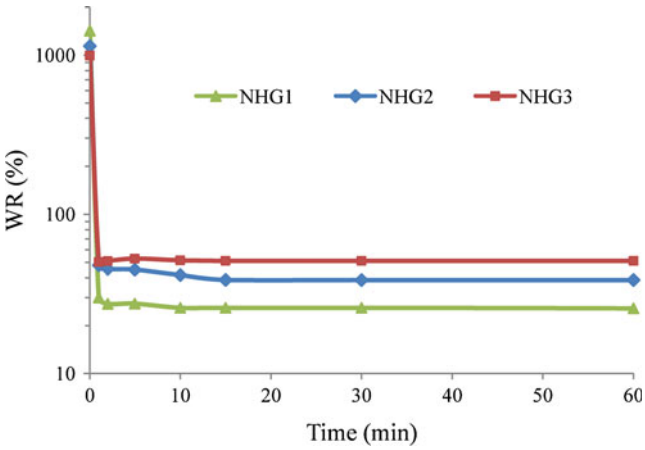

Fig. 7 Deswelling kinetics of NHG1–3 with different PVA contents of 0.5, 1, and 2 wt.%

42 °C. After each hydrogel had reached the ESR at 20 °C, it was quickly immersed in distilled water at 42 °C, at which point it began to shrink rapidly. As shown in Fig. 8, the nanohydrogels exhibit fast swelling/deswelling processes and good reversibilities. Therefore, the oscillating swelling/deswelling kinetics demonstrate that the nanohydrogels obtained in this work could be utilized as reversible thermoresponsive materials in many fields of biomedicine, bioengineering, and biotechnology [46].

Temperature and pH dependences of the swelling ratios of the nanohydrogels

The dependences of the swelling ratios (SRs) of the nanohydrogels NHG1–3 on temperature in the range 20–50 °C are shown in Fig. 9. The swelling ratio of each nanohydrogel decreases as the temperature of the nanohydrogel increases. The swelling curves show a characteristic decrease in the SR at about 30 °C, which is close to the LCSTs of the nanohydrogels as measured by DSC.

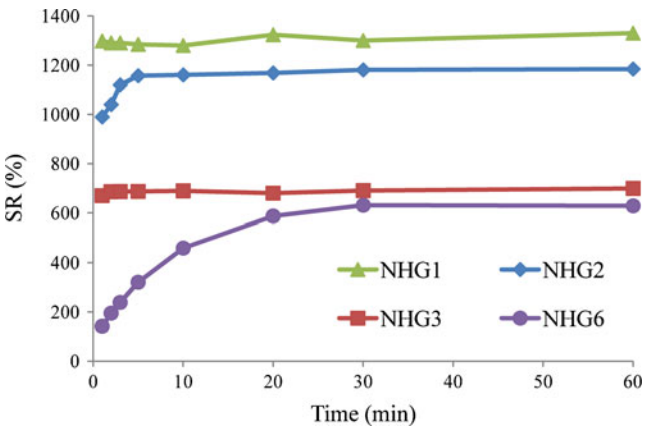

Fig. 6 Swelling kinetics of the PVA and NHG1–3 nanohydrogels with different PVA contents of 0.5, 1, and 2 wt.% at 25 °C

Below the LCST, the nanohydrogel is swollen because of the hydrophilicities of both PVA and PNIPAAm. As the temperature rises to the phase-transition temperature or the LCST, the hydrophobic interactions between the polymer chains become stronger than the polymer–water interactions, and the gel collapses [9]. The effect of pH on the swelling of the hydrogels is of great importance, as a change in the pH of the swelling medium often causes a fluctuation in the free volume accessible to penetrating water molecules, which affects the swelling properties of the hydrogels [29, 47]. Figure 10 illustrates the pH dependences of the swelling ratios of the nanohydrogels NHG1–3, which were immersed in a buffer solution at a pH in the range 2–10 at room temperature. As shown in Fig. 10, the equilibrium swelling ratio increases with increasing pH of the swelling medium. This can be explained by the fact that in the pH 2 and 4 buffer solutions, the amide groups in PNIPAAm form hydrogen bonds with the PVA chains, leading to small swelling ratios [48]. On the other hand, the PNIPAAm segments of the nanohydrogels undergo partial hydrolysis with increasing pH of the swelling medium, which prompts

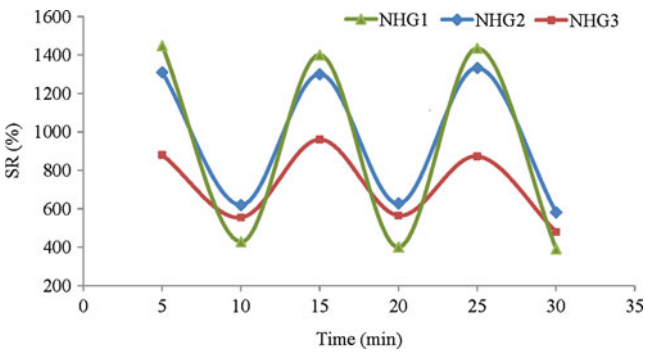

Fig. 8 Oscillating swelling–deswelling kinetics of the nanohydrogels NHG1–3 in response to the application of temperature cycles between 20 and 42 °C in water

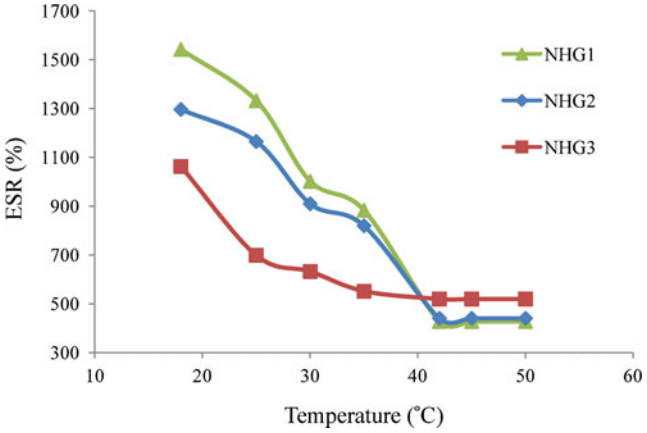

Fig. 9 Temperature dependences of the equilibrium swelling ratios for NHG1–3

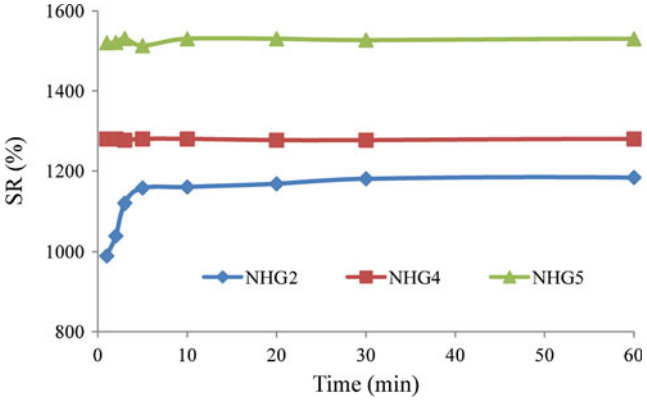

Fig. 11 The effect of initiator concentration on the swelling ratios of nanohydrogels (NHG2, NHG4, and NHG5 were synthesized with 10, 20, and 30 μL of H_2O_2)

the creation of anionic charged centers along the copolymeric chains. These polyelectrolyte chains cause repulsion between the macromolecular chains and thus enlarge the free volumes within the nanohydrogel network, which obviously enhances its water sorption capacity. However, as the pH increases further (pH 10), the ionic strength also increases, and the difference in the osmotic pressure of free ions between the internal and external solution decreases, which may inhibit the polymer–water interactions inside the nanohydrogel matrix, leading to deswelling of the nanohydrogel [29, 47–50].

Effect of initiator concentration on swelling behavior

Figure 11 presents the swelling ratios of nanohydrogels NHG2, NHG4, and NHG5, which were synthesized with 10, 20, and 30 μL of H_2O_2. As shown in Fig. 11, the swelling ratios of the nanohydrogels increase with increasing H_2O_2. Increasing the concentration of H_2O_2 increases the number of OH free radicals, which in turn increases the probability of the abstraction of hydrogen from the PVA backbone, causing more NIPAAm grafting [51]. These results are in accord with the elemental analysis data shown in Table 2, which indicate that the NIPAAm content in the final matrix increases slightly with increasing H_2O_2. Incorporating more NIPAAm into the PVA-*g*-NIPAAm nanohydrogel leads to an increase in the swelling ratio because of the hydrophilicity of PNIPAAm [22].

Cytotoxicity study

As nanohydrogels have potential applications in biomedical fields, a cytotoxicity study was performed to check the biocompatibility of the nanohydrogel NHG3 and its effects on cell viability. An MTT assay was used to determine cell viability following the nanohydrogel treatment. The results demonstrated that the nanohydrogel was nontoxic across the studied range of concentrations following 24 h of treatment, and that it did not have any significant effects on A549 cell viability (Fig. 12).

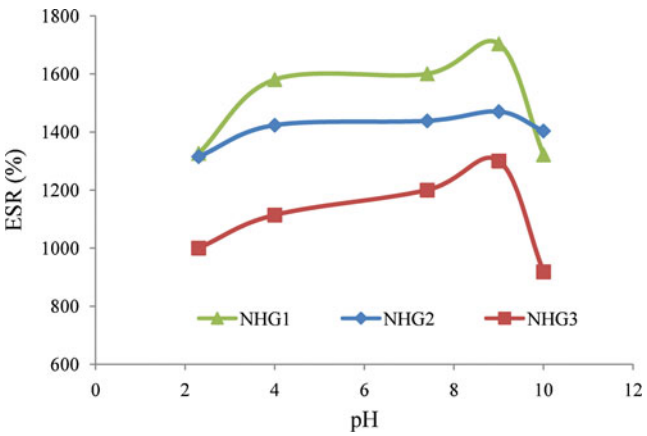

Fig. 10 Equilibrium swelling ratios at various pHs for NHG1–3

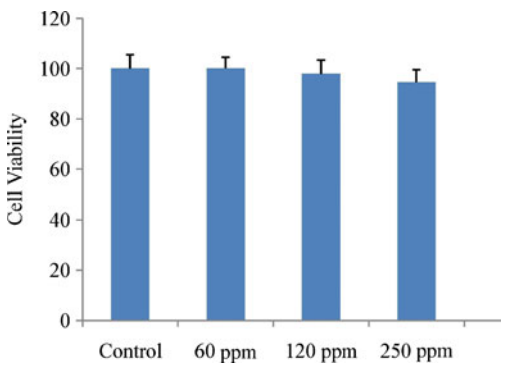

Fig. 12 Effects of the nanohydrogel NHG3 at different concentrations on cell survival

Conclusions

This report introduces a crosslinker-free method for the synthesis of PVA-*g*-NIPAAm nanohydrogels by intramolecular crosslinking in dilute aqueous solution at high temperature using H_2O_2 as an initiator. As a result, in dilute solution, where the distances between the macromolecules are large, and at temperatures above the LCST, the intramolecular crosslinking of the polymer chains and the association of collapsed hydrophobic PNIPAAm chains leads to nanohydrogel formation. TGA indicated that the thermal stability of PVA decreases due to NIPAAm grafting. A rheological investigation of the swollen nanohydrogels confirmed that they behave as viscoelastic solids, and their storage moduli were larger than their loss moduli across the entire frequency range tested. Swelling experiments indicated that the nanohydrogels show high water uptake and fast swelling/deswelling responses, and they show both temperature and pH sensitivity. The swelling ratios of the nanohydrogels increased as the contents of NIPAAm and H_2O_2 in the feed were increased. The results also demonstrated that the nanohydrogels undergo oscillatory swelling in response to changes in the temperature of the environment of the nanohydrogel. The biocompatibility of one of the nanohydrogels was confirmed in a cytotoxicity test. Finally, all of the results obtained reveal that the facile polymerization approach employed in this study yields nanohydrogels with great potential for use in drug-delivery systems.

Acknowledgment Financial support from the University of Tabriz is gratefully acknowledged.

References

1. Guerrero-Ramirez LG, Nuno-Donlucas SM, Cesteros LC, Katime I (2008) Mater Chem Phys 112:1088–1092
2. Yu Y, Li Y, Liu L, Zhu C, Xu Y (2011) J Polym Res 18:283–291
3. Li YY, Zhang XZ, Cheng H, Zhu JL, Cheng SX, Zhuo RX (2006) Macromol Rapid Commun 27:1913–1919
4. Jaiswal MK, Banerjee R, Pradhan P, Bahadur D (2010) Colloid Surface B 81:185–194
5. Hu J, Zheng S, Xu X (2012) J Polym Res 19:9988–9996
6. Wadajkar AS, Koppolu B, Rahimi M, Nguyen KT (2009) J Nanopart Res 11:1375–1382
7. Saikia AK, Mandal UK, Aggarwal S (2012) J Polym Res 19:9871–9879
8. Cheng CJ, Chu LY, Zhang J, Wang HD, Wei G (2008) Colloid Polym Sci 286:571–577
9. Zhang JT, Cheng SX, Zhuo RX (2003) Colloid Polym Sci 281:580–583
10. Zheng Y, Zheng S (2012) React Funct Polym 72:176–184
11. Mendrek S, Mendrek A, Adler HJ, Dworak A, Kuckling D (2009) Macromolecules 42:9161–9169
12. Griffin JM, Robb I, Bismarck A (2007) J Appl Polym Sci 104:1912–1919
13. Hennink WE, Nostrum CF (2002) Adv Drug Deliv Rev 54:13–36
14. Loh XJ, Peh P, Liao S, Sng C, Li J (2010) J Control Release 143:175–182
15. Gao J, Frisken BJ (2003) Langmuir 19:5217–5222
16. Gao J, Frisken BJ (2003) Langmuir 19:5212–5216
17. An JC (2010) J Ind Eng Chem 16:657–661
18. Ulanski P, Janik I, Kadlubowski S, Kozicki M, Kujawa P, Pietrzak M, Stasica P, Rosiac M (2002) Polym Adv Tech 13:951–959
19. Kadlubowski S, Grobelny J, Olejniczak W, Cichomski M, Ulanski P (2003) Macromolecules 36:2484–2492
20. Ulanski P, Janik I, Rosiak JM (1998) Radiat Phys Chem 52:289–294
21. Zhang JT, Bhat R, Jandt KD (2009) Acta Biomater 5:488–497
22. Kim SJ, Park SJ, Kim SI (2003) React Funct Polym 55:61–67
23. Diez-Pena E, Quijada-Garrido I, Barrales-Rienda JM (2002) Polymer 43:4341–4348
24. Wei H, Cheng SX, Zhang XZ, Zhuo RX (2009) Prog Polym Sci 34:893–910
25. Ghaemy M, Naseri M (2012) Carbohyd Polym 90:1265–1272
26. Shukla SK, Shaikh AW, Gunari N, Bajpai AK, Kulkarni RA (2009) J Appl Polym Sci 111:1300–1310
27. Schmidt T, Janik I, Kadlubowski S, Ulanski P, Rosiak JM, Reichelt R, Arndt KF (2005) Polymer 46:9908–9918
28. Rosiak JM, Janik I, Kadlubowski S, Kozicki M, Kujawa P, Stasica P, Ulanski P (2003) Nucl Instrum Meth B 208:325–330
29. Bajpai AK, Bajpai J, Shukla S (2001) React Funct Polym 50:9–21
30. Bajpai AK, Gupta R (2010) Polym Compos 31:245–255
31. Morimoto N, Qiu XP, Winnik FM, Akiyoshi K (2008) Macromolecules 41:5985–5987
32. Peppas NA, Scutt JE (1992) J Control Release 18:95–100
33. Lozinsky VI (1998) Russ Chem Rev 67:573–586
34. Maolin Z, Ning L, Jun L, Min Y, Jiuqiang L, Hongfei H (2000) Radiat Phys Chem 57:481–484
35. Constantin M, Fundueanu G (2009) Rev Roum Chim 54:1031–1039
36. Zhao S, Cao M, Li H, Li L, Xu W (2010) Carbohyd Res 345:425–431
37. Sheikh A, Barakat NAM, Kanjwal MA, Aryal S, Khil MS, Kim HY (2009) J Mater Sci Mater M 20:821–831
38. Mu Q, Fang Y (2008) Carbohyd Polym 72:308–314
39. Ogata T, Nonaka T, Kurihara S (1995) J Mem Sci 103:159–165
40. Lee BH, Vernon B (2005) Macromol Biosci 5:629–635
41. Dumitriu RP, Mitchell GR, Vasile C (2011) Polym Int 60:1398–1407
42. Hsu Sh YTL (2000) Macromol Rapid Commun 21:476–480
43. Wang Q, Zhao Y, Yang Y, Xu H, Yang X (2007) Colloid Polym Sci 285:515–521
44. Zhang JT, Cheng SX, Huang SW, Zhuo RX (2003) Macromol Rapid Commun 24:447–451
45. Safrany A (2005) Nucl Instrum Meth B 236:587–593
46. Liu M, Su H, Tan T (2012) Carbohyd Polym 87:2425–2431
47. Lakouraj MM, Tajbakhsh M, Mokhtary M (2005) Iran Polym J 14:1022–1030
48. Lee YM, Kim SH, Choz CS (1996) J Appl Polym Sci 62:301–311
49. Jianqi F, Lixia G (2002) Eur Polym J 38:1653–1658
50. Kim SJ, Park SJ, Lee SM, Lee YM, Kim HC, Kim SI (2003) J Appl Polym Sci 89:890–894
51. Lanthong P, Nuisin R, Kiatkamjornwong S (2006) Carbohyd Polym 66:229–245